



Cite this: *Chem. Commun.*, 2019, 55, 3939

Received 29th January 2019,
Accepted 1st March 2019

DOI: 10.1039/c9cc00831d

rsc.li/chemcomm

Unusual temperature-promoted carbon dioxide capture in deep-eutectic solvents: the synergistic interactions†

Shashi Kant Shukla *^a and Jyri-Pekka Mikkola*^{ab}

A series of novel ethylenediamine (EDA)-based deep-eutectic solvents (DESSs) gave rise to unexpectedly large carbon dioxide (CO₂) capture capacities at higher temperatures owing to the “synergistic interaction” between the donor and acceptor moieties.

Reversible fixation–release of carbon dioxide (CO₂) has attracted much attention during the last few decades due to an excessive increase in the consumption of fossil fuels as the main source of energy, thus causing an upsurge in CO₂ emissions, leading to global warming. The current state-of-the-art industrial technology uses amine-based solvents in reversible CO₂ capture.¹ This methodology has critical issues such as high regeneration energy, amine instability, high volatility, corrosion and high maintenance costs.^{2,3} In order to optimize the CO₂ uptake, the flue gas is cooled to room temperature before absorption, whereas high temperatures are required in the desorption–regeneration step. Both these steps increase the cost of the setup and hence developing a solvent system that can absorb CO₂ directly from hot flue gas and undergo rapid desorption is the most attractive solution but have not been introduced until now.

The last century witnessed a surge in the development of a number of “green and sustainable” alternatives to volatile solvents. Among them, ionic liquids (ILs) and deep-eutectic solvents (DESSs) have been the most explored ones for various applications because of their advantageous properties such as their negligible vapour pressure, wide liquidus range, low flammability, high thermal stability and recyclability.^{4,5} Blanchard *et al.* reported for the first time the potential of ILs in CO₂ capture.⁶

Later, various ILs differing in terms of cations, anions and alkyl chain length were applied to optimize CO₂ uptake and to gain understanding about the functioning of these neoteric media.^{7–10} The basicity of the anion was identified as the key factor in achieving high CO₂ uptake and has been most explored to date.^{11–14} For example, in carbonyl-containing anion-functionalized ILs, high CO₂ intake was favoured by H-bonding interactions.¹⁵ Pan *et al.* reported an equimolar CO₂ uptake in anion-functionalized hydroxypyridine-based ILs owing to intramolecular proton transfer.¹⁶ However, the high molar uptake in ILs is attributed to their large molar mass and thus is less impressive when converted to the gravimetric values.^{10,17} Similarly, task-specific ILs for CO₂ capture are expensive and require a long time for synthesis and are therefore rendered unsuitable for industrial applications.¹⁸

In contrast, DESSs, a new generation of solvent analogous to ILs, provide a more promising alternative in CO₂ capture and involve cost-effective, easy preparation, exhibiting properties similar to ILs, and resulting in higher gravimetric CO₂ uptake.^{19,20} In a short time-span, DESSs have found application in organic synthesis, polymerization, stabilization of biomolecules, nanotechnology, separation, extraction of target compounds and so on.^{21–26} The performance of DESSs as sorbents in CO₂ capture relies on pairing an efficient hydrogen bond donor (HBD) with hydrogen bond acceptor (HBA) with an optimal molar ratio.^{27–29} Later developments have shown moderate to high CO₂ uptakes for different classes of DESSs.^{30–33} We recently presented an in-depth discussion about the impact of intermolecular interactions on the CO₂ uptake in ethylenediamine ([EDA])- , 3-amino-1-propanol ([AP])- , and polyamine-based DESSs.³³ Unlike ILs and amine-based solvent systems where basicity is a prerequisite for high CO₂ capture, the interplay between the hydrogen bond donor acidity (α) and hydrogen bond acceptor basicity (β) governs the CO₂ absorption in DESSs.³³ Additionally, the reaction conditions also influence the CO₂ solubility and maximum uptake takes place at low temperatures and high pressures.³⁴ In line with the current technology, flue gas passes through a cooler before traveling to the absorption tank.³⁵ Therefore, employing

^a Technical Chemistry, Department of Chemistry, Chemical-Biological Centre, Umeå University, SE-90187 Umeå, Sweden. E-mail: shashi.kant.shukla@umu.se, jyri-pekka.mikkola@umu.se

^b Industrial Chemistry & Reaction Engineering, Department of Chemical, Engineering, Johan Gadolin Process Chemistry Centre, Åbo Akademi University, FI-20500 Åbo-Turku, Finland

† Electronic supplementary information (ESI) available: Tables and figures, synthesis and characterization of DESSs, polarity, viscosity, activation energy of viscous flow and thermodynamic characterization, and temperature-dependent CO₂ capture profiles. See DOI: 10.1039/c9cc00831d



a medium that has a low enthalpy of absorption (ΔH_{abs}) and can reversibly absorb CO_2 in the post-combustion process, at typical flue gas temperatures, will eliminate the necessity of a cooler unit and extra steam (for desorption), thus bringing down the cost of the overall setup and making the whole process more lucrative.

In this study, we synthesized DESs containing [EDA], [AP], diethylenetriamine ([DETA]), tetraethylenepentamine ([TEPA]) and pentaethylenhexamine ([PEHA]) as HBDs and monoethanolammonium chloride ([MEA-Cl]) and 1-methylimidazolium chloride ([HMIM-Cl]) as their HBA counterparts (see the ESI† for details) and measured the CO_2 uptakes at temperatures 298 K–328 K, at ambient pressure (Table 1). The structures of the different DESs are shown in Fig. 1. As depicted in Fig. 2 and 3, respectively, the [EDA]- and [AP]-based DESs have opposite CO_2 uptake behaviours within the same temperature range. The [EDA]-based DESs show a positive trend in terms of temperature, while a negative temperature effect is evident for the [AP]-class of DESs. So far, only a negative impact of increasing temperatures on CO_2 capture has been perceived in previous investigations.^{32,35,36}

As shown in Fig. 2, the gravimetric CO_2 uptake increases from 11.4% to 24.8% in 1 : 1 [MEA-Cl][EDA] and 3.6% to 12.1% in 1 : 1 [HMIM-Cl][EDA], respectively, in the temperature range

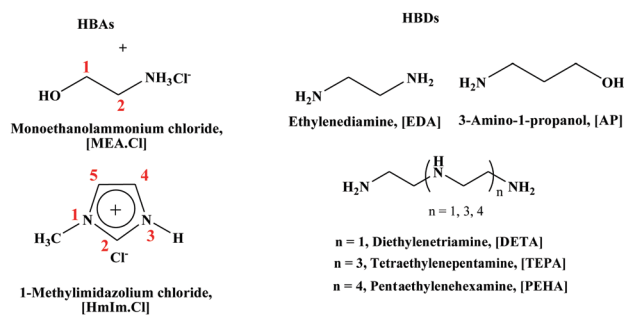


Fig. 1 Structures of DESs.

Table 1 Activation energies of viscous flow, and thermodynamic and polarity parameters in [EDA]- and [AP]-based DESs

DESs	$E_{a,\eta}$	ΔH°	ΔS°	E_{T30}	α	β
[MEA-Cl][EDA] = 1 : 1	42.7	11.9	4.3	59.2	0.948	0.688
[MEA-Cl][EDA] = 1 : 2	42.4	10.8	4.0	56.5	0.785	0.681
[MEA-Cl][EDA] = 1 : 3	42.2	8.0	3.1	54.6	0.673	0.658
[MEA-Cl][EDA] = 1 : 4	41.8	7.3	2.9	53.2	0.599	0.791
[HMIM-Cl][EDA] = 1 : 1	48.0	17.0	5.7	54.7	—	—
[HMIM-Cl][EDA] = 1 : 2	42.1	7.9	3.0	54.7	0.653	0.615
[HMIM-Cl][EDA] = 1 : 3	38.9	7.2	2.9	53.9	0.646	0.861
[HMIM-Cl][EDA] = 1 : 4	38.8	7.1	2.8	52.7	0.613	0.901
[MEA-Cl][AP] = 1 : 1	48.3	−10.0	−4.5	60.2	1.013	0.526
[MEA-Cl][AP] = 1 : 2	47.3	−8.6	−3.7	59	1.045	0.628
[MEA-Cl][AP] = 1 : 3	43.0	−7.5	−3.1	58	0.932	0.696
[MEA-Cl][AP] = 1 : 4	35.6	−6.6	−2.8	57.2	0.895	0.720
[HMIM-Cl][AP] = 1 : 1	49.3	−25.2	−12.5	59.2	1.000	0.631
[HMIM-Cl][AP] = 1 : 2	43.2	−9.1	−4.5	58.1	0.941	0.629
[HMIM-Cl][AP] = 1 : 3	42.7	−8.0	−3.6	57.4	0.910	0.720
[HMIM-Cl][AP] = 1 : 4	39.8	−5.8	−2.6	56.6	0.869	0.713

$E_{a,\eta}$ = kJ mol^{−1}, ΔH° = kJ mol^{−1}, ΔS° = J K^{−1} mol^{−1}, $E_{T(30)}$ = kcal mol^{−1}; the error in $E_{a,\eta}$, ΔH° , ΔS° and $E_{T(30)}$ are ± 0.003 , ± 0.002 , ± 0.001 and 0.004, respectively.

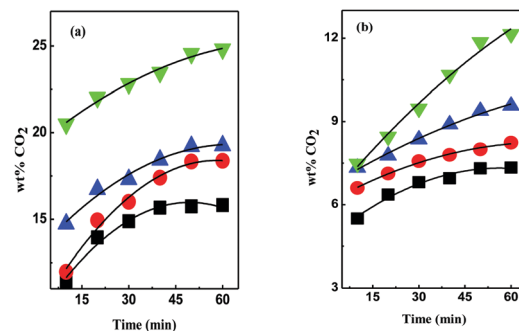


Fig. 2 CO_2 uptake kinetics in 1 : 1 (a) [MEA-Cl][EDA]- and (b) [HMIM-Cl][EDA]-based DESs at 298 K (■), 308 K (●), 318 K (▲) and 328 K (▼).

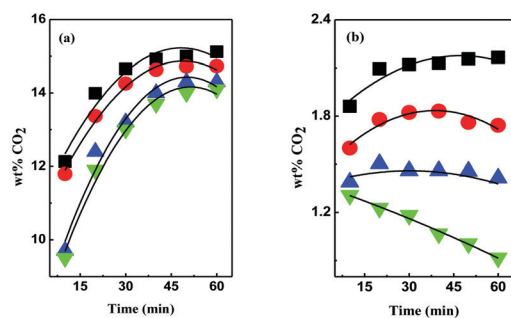


Fig. 3 CO_2 uptake kinetics in 1 : 1 (a) [MEA-Cl][AP]- and (b) [HMIM-Cl][AP]-based DESs at 298 K (■), 308 K (●), 318 K (▲) and 328 K (▼).

298 K–328 K in 1 h. The CO_2 capture capacity increases further upon increasing the HBA : HBD ratio from 1 : 1 to 1 : 4. In 1 : 4 [MEA-Cl][EDA], the CO_2 uptake reaches $\sim 36\%$ in 1 h at 328 K, whereas in 1 : 4 [HMIM-Cl][EDA] $\sim 34\%$ of CO_2 is sorbed at 328 K (ESI,† Fig. S1–S4). Contrary to our reports, Trivedi *et al.* reported lower CO_2 uptake in 1 : 3 [MEA-Cl][EDA] at a higher temperature, which is surprising to us.³² The temperature-promoted CO_2 uptake was not specific to the [EDA]-based DESs noted in [DETA]-, [TEPA]- and [PEHA]-based DESs; though, the efficiency was lower than in the former case (ESI,† Fig. S5 and S6).

In general, an increasing temperature results in a lower viscosity but increases the activation energy of the gas molecule at the same time. The resultant of these opposing effects directs the course of CO_2 capture, at higher temperatures. Therefore, the temperature-favoured CO_2 uptake in the [EDA]-based DESs cannot be attributed to the reduction in viscosity only. Additionally, [MEA-Cl][EDA] and [HMIM-Cl][EDA] possess low viscosity, which further decreases upon increasing the HBA : HBD ratio from 1 : 1 to 1 : 4. In the latter case, the viscosity is already low so the influence of temperature is hard to detect. To discern the impact of viscosity on CO_2 uptake more clearly, we calculated the activation energy of viscous flow ($E_{a,\eta}$) from the temperature-dependent viscosity data using the Arrhenius-type equation (ESI,† Fig. S7) as shown in Table 1. $E_{a,\eta}$ accounts for the hindrance in the diffusion of CO_2 by the DES. At HBA : HBD = 1 : 1, the [EDA]-based DESs possess lower $E_{a,\eta}$ than the [AP]-class of DESs but, at higher HBA : HBD ratios, the trend in $E_{a,\eta}$ reverses (Table 1). The $E_{a,\eta}$ values of the [DETA], [TEPA] and [PEHA]-based DESs vary



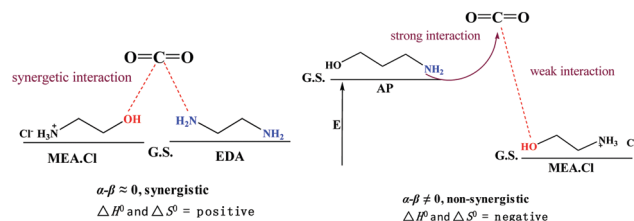
between 43.2 and 60.6 kJ mol⁻¹ despite the positive effect of temperature on CO₂ capture (ESI,† Table S1). Thus, the positive and negative temperature effects on the CO₂ solubility in the [EDA]- and [AP]-based DESs, respectively, might originate from the different intermolecular interactions between the DESs and CO₂.

To account for the impact of intermolecular interactions on the course of CO₂ capture, at elevated temperatures, the thermodynamics (standard enthalpy change (ΔH°) and standard entropy change (ΔS°)) of capture along with the solvent polarity parameters ($E_T(30)$, α and β) are discussed further to unravel the underlying mechanisms^{33,37} (see the ESI,† Fig. S8 and S9 and Table S2).

As shown in Table 1, a positive ΔH° for the [EDA]-based DESs indicates an endothermic nature of CO₂ uptake, while a negative ΔH° for the [AP]-based DESs signals that the process is exothermic. The standard entropy change (ΔS°) is positive for the [EDA]-class and negative for the [AP]-class of DESs. Following the spontaneity criteria ($\Delta G^\circ = \Delta H^\circ - T\Delta S^\circ$), it is evident that the CO₂ uptake becomes more spontaneous ($-T\Delta S^\circ > \Delta H^\circ$) in [MEA·Cl][EDA] and [HMIM·Cl][EDA] than [MEA·Cl][AP] and [HMIM·Cl][AP] as the temperature increases. A shift in HBA:HBD from 1:1 to 1:4 decreases ΔH° and ΔS° in the [EDA]-based DESs and thus renders CO₂ uptake more spontaneous. In the [AP]-class of DESs with an increase of the HBA:HBD ratio, ΔH° and ΔS° become less negative and thus spontaneous and result in higher CO₂ uptake. The [DETA]-, [TEPA]- and [PEHA]-based DESs have positive ΔH° and ΔS° akin to the [EDA]-class of DESs and hence dissolve CO₂ spontaneously as the temperature increases (ESI,† Table S1). More importantly, a very small value of ΔH° for the [EDA]-based DESs makes regeneration of the absorbent energy-saving, which is a key factor in practical applications.³⁸

The nature of DES–CO₂ interactions was then investigated in terms of the Kamlet–Taft parameters α and β , which measure donor and acceptor strengths, respectively (ESI,† Table S2 and Fig. S10). The positive effect of CO₂ uptake indicates “synergistic interaction” of the donor and acceptor sites in the [EDA]-based DESs. The synergistic action is widely acknowledged in catalysis and polarity measurements of binary systems.^{39,40} “Hyperpolarity” was observed in a binary mixture of ILs when the donor (α) and acceptor (β) strengths become similar and favour synergistic interaction.⁴¹ In other words, for synergistic interaction, the relative difference between the donor and acceptor ($\alpha - \beta$) should be zero. If $\alpha - \beta \neq 0$, the system will have acidic/basic characteristics depending on the relative differences in the values of α and β . This will cause an energy difference in the HBA and HBD in a DES and lower the probability for synergistic interactions (Scheme 1). The synergy in the DES results in weak interactions, which is reflected in the low polarity ($E_T(30)$) and ΔH° and ΔS° values.

As shown in Table 1, the relative $\alpha - \beta$ for [MEA·Cl][EDA] is lower than those of [MEA·Cl][AP] and [HMIM·Cl][AP] at 1:1. The small $\alpha - \beta$ suggests alignment of the donor and acceptor energy levels for synergistic interactions. At higher HBA:HBD ratios, in the [EDA]-based DESs, relative $\alpha - \beta$ nears zero and renders the synergistic interactions more feasible. Decreases in the ΔH° and ΔS° further support this trend. Similarly, the $\alpha - \beta$



Scheme 1 Representation of synergistic and non-synergistic interactions and thermodynamic criteria in DESs.

trend in the [HMIM·Cl][EDA]-class of DESs also indicates synergistic interactions at different molar ratios. The relative $\alpha - \beta$ for the [AP]-class of DESs is comparatively large and hence results in negative ΔH° and ΔS° (Table 1). The large $\alpha - \beta$ gives rise to differences in the ground state energy of the donor and acceptor and forbids synergistic interactions (Scheme 1). Thus, the greater CO₂ uptake in the [AP]-class of DESs, at higher HBA:HBD ratios, is due to their reduced viscosity.

The [DETA]-, [TEPA]- and [PEHA]-based DESs possess large $\alpha - \beta$ but have positive ΔH° and ΔS° , which suggests the possibility of synergistic interactions. The large in $\alpha - \beta$ difference is caused by the multiple amine groups in the HBDs.

In summary, we, for the first time, have reported temperature-promoted CO₂ capture in novel [EDA]-based DESs. The positive effect of temperature on CO₂ capture arises from the synergistic interactions between the donor and acceptor moieties. The synergistic interactions in DESs are caused by small $\alpha - \beta$ and $E_T(30)$ and positive ΔH° and ΔS° . Lower CO₂ uptake in the [AP]-class of DESs, at elevated temperatures, is due to the large $\alpha - \beta$ and negative ΔH° and ΔS° . Very low ΔH° indicates quick regeneration of the [EDA]-based DESs and hence these DESs evolve as excellent substitutes for the amine-based technology in a CO₂ capture plant.

We are thankful to the Wallenberg Wood Science Center (WWSC), Kempe Foundations, and the Bio4Energy programme. This work is also part of the activities of the Johan Gadolin Process Chemistry Centre at Åbo Akademi University.

Conflicts of interest

There are no conflicts to declare.

References

- G. T. Rochelle, *Science*, 2009, **325**, 1652–1654.
- R. López-Rendón, M. A. Mora, J. Alejandro and M. E. Tuckerman, *J. Phys. Chem. B*, 2006, **110**, 14652–14658.
- S. Zeng, X. Zhang, L. Bai, X. Zhang, H. Wang, J. Wang, D. Bao, M. Li, X. Liu and S. Zhang, *Chem. Rev.*, 2017, **117**, 9625–9673.
- X. P. Zhang, X. C. Zhang, H. F. Dong, Z. J. Zhao, S. J. Zhang and Y. Huang, *Energy Environ. Sci.*, 2012, **5**, 6668–6681.
- Q. R. Sheridan, W. F. Schneider and E. J. Maginn, *Chem. Rev.*, 2018, **118**, 5242–5260.
- L. A. Blanchard, D. Hancu, E. J. Beckman and J. F. Brennecke, *Nature*, 1999, **399**, 28–29.
- B. E. Gurkan, J. C. de la Fuente, E. M. Mindrup, L. E. Ficke, B. F. Goodrich, E. A. Price, W. F. Schneider and J. F. Brennecke, *J. Am. Chem. Soc.*, 2010, **132**, 2116–2117.



- 8 Y. Q. Zhang, S. J. Zhang, X. M. Lu, Q. Zhou, W. Fan and X. P. Zhang, *Chem. – Eur. J.*, 2009, **15**, 3003–3011.
- 9 C. M. Wang, X. Y. Luo, H. M. Luo, D. E. Jiang, H. R. Li and S. Dai, *Angew. Chem., Int. Ed.*, 2011, **50**, 4918–4922.
- 10 C. M. Wang, H. M. Luo, D. E. Jiang, H. R. Li and S. Dai, *Angew. Chem., Int. Ed.*, 2010, **49**, 5978–5981.
- 11 I. Niedermaier, M. Bahlmann, C. Papp, C. Kolbeck, W. Wei, S. K. Calderon, M. Grabau, P. S. Schulz, P. Wasserscheid, H. P. Steinruck and F. Maier, *J. Am. Chem. Soc.*, 2014, **136**, 436–441.
- 12 B. F. Goodrich, J. C. de la Fuente, B. E. Gurkan, D. J. Zadigian, E. A. Price, Y. Huang and J. F. Brennecke, *Ind. Eng. Chem. Res.*, 2011, **50**, 111–118.
- 13 C. M. Wang, H. M. Luo, X. Y. Luo, H. R. Li and S. Dai, *Green Chem.*, 2010, **12**, 2019–2023.
- 14 T. Oncsik, R. Vijayaraghavan and D. R. MacFarlane, *Chem. Commun.*, 2018, **54**, 2106–2109.
- 15 F. Ding, X. He, X. Luo, W. Lin, K. Chen, H. Lia and C. Wang, *Chem. Commun.*, 2014, **50**, 15041–15044.
- 16 M. Pan, R. Vijayaraghavan, F. Zhou, M. Kar, H. Li, C. Wang and D. R. MacFarlane, *Chem. Commun.*, 2017, **53**, 5950–5953.
- 17 E. D. Bates, R. D. Mayton, I. Ntai and J. H. Davis, *J. Am. Chem. Soc.*, 2002, **124**, 926–927.
- 18 B. Gurkan, B. F. Goodrich, E. M. Mindrup, L. E. Ficke, M. Massel, S. Seo, T. P. Senftle, H. Wu, M. F. Glaser, J. K. Shah, E. J. Maginn, J. F. Brennecke and W. F. Schneider, *J. Phys. Chem. Lett.*, 2010, **1**, 3494–3499.
- 19 A. P. Abbott, G. Capper, D. L. Davies, H. L. Munro, R. K. Rasheed and V. Tambyrajah, *Chem. Commun.*, 2001, 2010–2011.
- 20 A. Zhu, T. Jiang, B. Han, J. Zhang, Y. Xie and X. Ma, *Green Chem.*, 2007, **9**, 169–172.
- 21 A. Abo-Hamad, M. Hayyan, M. A. H. AlSaadi and M. A. Hashim, *Chem. Eng. J.*, 2015, **273**, 551–567.
- 22 B. Tang, H. Zhang and K. H. Row, *J. Sep. Sci.*, 2015, **38**, 1053–1064.
- 23 J. García-Álvarez, *Eur. J. Inorg. Chem.*, 2015, 5147–5157.
- 24 F. del Monte, D. Carriazo, M. C. Serrano, M. C. Gutierrez and M. L. Ferrer, *ChemSusChem*, 2014, **7**, 999–1009.
- 25 H. Zhao, *J. Chem. Technol. Biotechnol.*, 2015, **90**, 19–25.
- 26 C. Vidal, J. García-Álvarez, A. Hernán-Gómez, A. R. Kennedy and E. Hevia, *Angew. Chem., Int. Ed.*, 2016, **55**, 16145–16148.
- 27 Q. H. Zhang, K. D. Vigier, S. Royer and F. Jerome, *Chem. Soc. Rev.*, 2012, **41**, 7108–7146.
- 28 M. Francisco, A. van den Bruinhorst and M. C. Kroon, *Angew. Chem., Int. Ed.*, 2013, **52**, 3074–3085.
- 29 Y. Dai, J. van Spronsen, G.-J. Witkamp, R. Verpoorte and Y. H. Choi, *J. Nat. Prod.*, 2013, **76**, 2162–2173.
- 30 X. Li, M. Hou, B. Han, X. Wang and L. Zou, *J. Chem. Eng. Data*, 2008, **53**, 548–550.
- 31 M. Francisco, A. van den Bruinhorst, L. F. Zubeir, C. J. Peters and M. C. Kroon, *Fluid Phase Equilib.*, 2013, **340**, 77–84.
- 32 T. J. Trivedi, J. H. Lee, H. J. Lee, Y. K. Jeong and J. W. Choi, *Green Chem.*, 2016, **18**, 2834–2842.
- 33 S. K. Shukla and J.-P. Mikkola, *Phys. Chem. Chem. Phys.*, 2018, **20**, 24591–24601.
- 34 S. Sarmad, Y. Xie, J.-P. Mikkola and X. Jia, *New J. Chem.*, 2017, **41**, 290–301.
- 35 I. Kim and H. F. Svendsen, *Ind. Eng. Chem. Res.*, 2007, **46**, 5803–5809.
- 36 A. Finotello, J. E. Bara, D. Camper and R. D. Noble, *Ind. Eng. Chem. Res.*, 2008, **47**, 3453–3459.
- 37 S. K. Shukla and A. Kumar, *J. Phys. Chem. B*, 2015, **119**, 5537–5545.
- 38 J. Ren, L. Wu and B.-G. Li, *Ind. Eng. Chem. Res.*, 2013, **52**, 8565–8570.
- 39 K. Herodes, I. Leito, I. Koppel and M. Rosés, *J. Phys. Org. Chem.*, 1999, **12**, 109–115.
- 40 L. Hongliang, W. Liangbing, D. Yizhou, P. Zhengtian, L. Zhuhan, C. Yawei, W. Menglin, Z. Xusheng, Z. Junfa, Z. Wenhua, S. Rui, M. Chao and Z. Jie, *Nat. Nanotechnol.*, 2018, **13**, 11–417.
- 41 A. Sarkar, S. Trivedi, G. A. Baker and S. Pandey, *J. Phys. Chem. B*, 2008, **112**, 14927–14936.

